

Environmental drivers and sources of stream oxygen consumption in an agricultural lake catchment

Jonas Stage Sørensen^{*,1}, Theis Kragh¹, Kaj Sand-Jensen, Kenneth Thorø Martinsen

University of Copenhagen, Universitetsparken 4, 3. floor, 2100 Copenhagen, Denmark

ARTICLE INFO

Keywords:

Stream
Oxygen consumption
Oxygen depletion
Climate change
Organic material
Eutrophication
PARAFAC
Agriculture

ABSTRACT

The combination of ongoing climate change and the historical loss of streams and wetland areas have presented new ecological challenges. These challenges became evident during a massive fish kill in Lake Fil, Denmark, in August 2018. We know that high amounts of labile organic matter entered the lake after a particularly heavy rainfall that followed a long period of heat and drought. Bacteria decomposed the organic matter, resulting in a quickly deoxygenated lake and an extensive fish kill. However, we do not know whether there is spatial variation in the amount of transportable labile matter across the catchment area. Identifying catchment 'hotspots' that sustain particularly high oxygen consumption rates will help managers to pursue interventions that can promote a high ecological quality of Lake Fil and its catchment. The method we developed to identify hotspots can be used by practitioners everywhere to prepare for and mitigate events similar to the 2018 disaster at Lake Fil. To identify hotspots in the stream network that feeds into Lake Fil, we measured oxygen consumption rates and environmental variables at 13 sites on five occasions. We found that oxygen consumption rates varied 2–16-fold between sites and 2–13-fold between sampling days. Oxygen consumption rates were positively related to the concentration of tryptophan-like material and ammonium but negatively related to the complexity of humic substances. Together, these variables accounted for 65% of the variation in the oxygen consumption rate across sub-catchments. High levels of tryptophan-like material and dissolved nutrients derive from intensive agricultural land use in the catchment. However, all oxygen consumption rates measured in this paper were apparently lower than those during the fish kill of August 2018, when the catchment fed higher concentrations of labile organic matter into the lake. The risk of anoxic water and fish kills can be mitigated by reducing and dispersing the input of labile organic matter following shifting periods of drought and heavy rain, which can be done by creating wetlands in the stream network or by implementing biogas facilities, thereby reducing pulses of organic matter and nutrients entering the stream.

1. Introduction

Three centuries of anthropogenic influence have subjected freshwater ecosystems to eutrophication, organic pollution, and conversion of natural areas to farmland (Biggs et al., 2017; Dahl, 1990, 2011; Dudgeon et al., 2006; Verhoeven et al., 2006). Active pumping to lower the groundwater level combined with channelization and piping of streams have ensured drainage and enabled the cultivation of two-thirds of Denmark's wetland area over the past 200 years (Brookes, 1987; Hansen, 2008; Neilsen, 2002). The use of fertilizers and imported fodder increased the surplus of nitrogen and phosphorus in industrialized agricultural systems, and leakages affected the dynamics of the

surrounding terrestrial and aquatic ecosystems (Smith, 2003).

Emergent climate change threatens freshwater ecosystems with physical, chemical, and biological effects (Reid et al., 2019). Predictions of future climate scenarios in Northern Europe include higher average inland water temperature and a greater prevalence of events that now are considered both extreme and unusual: heatwaves and droughts; extreme rain and flooding. Higher water temperature results in faster microbial activity and an increase in the metabolism of plants and animals, thus increasing the demand for oxygen. However, higher water temperatures are also associated with lower oxygen solubility, meaning that these ecosystems will face challenges even in the best of global-warming scenarios (Elliott, 1994; Sand-Jensen and Frost-Christensen,

* Corresponding author.

E-mail address: jonassoe@biology.sdu.dk (J.S. Sørensen).

¹ Present address: University of Southern Denmark, Campusvej 55, 5230 Odense M, Denmark.

1998; Sand-Jensen and Pedersen, 2005; Thyssen et al., 1987). Droughts make soil and other surface materials more vulnerable to being transported through runoff (Larned, 2000). Thus, more frequent droughts and high precipitation events are expected to increase markedly and could lead to flooding of lowland soils and higher allochthonous input from catchment areas into streams and lakes (Iversen et al., 1982). During the summer of 2018, an intensive drought followed by extreme rainfall had extraordinary consequences. Denmark's hottest and driest May, June, and July on record was followed by a heavy thunderstorm that flushed labile dissolved organic matter (DOM) into Lake Fil, where microbial oxygen consumption became exceptionally high. The southern lake basin turned anoxic within a few days, and virtually the entire fish population suffocated (Kragh et al., 2020). With global warming and the increasing frequency and intensity of extreme weather, it is reasonable to expect recurring anoxic events and fish kills in freshwater ecosystems. Some events may follow the Lake Fil trajectory; others may follow different trajectories. The impact of such events can be minimized by effective management of freshwater systems. New threats, like the one seen at Lake Fil in August 2018, motivated us to identify potential hotspots in the catchment that contribute to water with high oxygen consumption rates. In doing so, solutions for future management efforts to avoid repeated fish kills can be obtained. The process by which Lake Fil became oxygen-depleted is fairly well understood but nonetheless requires a brief explanation to understand our approach to identifying hotspots of impact.

The oxygen consumption rate in stream water is influenced by variables such as the concentration and lability of DOM, water temperature, and inorganic nutrients regulating the numbers and specific activity of heterotrophic bacteria (Pedersen and Sand-Jensen, 2007; Peters et al., 1987; Sand-Jensen and Pedersen, 2005; Sand-Jensen et al., 2007; Wetzel, 2001). It is well-known that microbial respiration increases with temperature across a range from approximately 0 to 35 °C (Johnson et al., 1974). Furthermore, the combination of increased temperature and inorganic nutrient concentration increases bacterial biomass and respiration (Ferreira et al., 2015; Fierer et al., 2005; Meyer and Johnson, 1983; Peters et al., 1987; White et al., 1991).

DOM and CDOM (colored DOM) influence light absorbance, vertical temperature structure, microbial activity, and oxygen conditions in aquatic systems (Sankar et al., 2020; Stedmon et al., 2003). One way to measure the specific characteristics of DOM is through fluorescence emission spectroscopy and statistical separation of the components using parallel factor analysis (PARAFAC). These techniques can be applied to identify labile and recalcitrant DOM components (Murphy et al., 2013) and have previously been used to characterize catchment land use (Sankar et al., 2020). DOM with high proportions of tryptophan-like material (hereafter denoted as tryptophan) is a proxy for human impact. Tryptophan has been shown in earlier studies to correlate positively with the oxygen consumption rate (Baker and Inverarity, 2004; Hudson et al., 2008). Consequently, in sub-catchments with intensively cultivated agricultural areas or other forms of extensive human impact, high export of tryptophan-related compounds may increase the oxygen consumption rate within streams (Ahmad and Reynolds, 1999; Baker and Curry, 2004; Baker and Inverarity, 2004; Comber et al., 1996; Hudson et al., 2008; Reynolds, 2002; Reynolds and Ahmad, 1997).

Bacterial decomposition rate depends partly on the concentration of labile organic material (Allan and Castillo, 2007; Peters et al., 1987). Sources of organic material in aquatic ecosystems are highly variable in both space and time. Streams in agricultural areas show elevated DOM content during high precipitation events in summer (Sand-Jensen and Pedersen, 2005). Exceptionally high organic material inputs can be expected if the application of liquid manure on agricultural fields is quickly followed by intensive rain and runoff.

CDOM is usually highly refractory due to its origin from the degradation of terrestrial plants. Furthermore, it is low in nitrogen (N) and particularly low in phosphorus (P) relative to carbon. Thus, the CDOM

proportion of DOM and the complexity of CDOM can indicate the lability of the DOM that enters a stream (Hopkinson Jr et al., 2002; Ogura, 1972; Søndergaard et al., 1995). The absorbance of UV-light at 254 nm relative to the dissolved organic carbon (DOC) concentration, the SUVA index, is a measure of DOM's lability (Weishaar et al., 2003). The SUVA index is lower in newly produced and thus more labile DOM than in old DOM that has become more aromatic and recalcitrant through degradation. Thus, SUVA serves as a predictor of oxygen consumption rate (Figueroa-Nieves et al., 2014).

The overall objectives of this study were to identify environmental variables and track the primary sources affecting oxygen consumption in the catchment area of Lake Fil, Denmark. The specific objectives were to 1) determine key drivers of variation in oxygen consumption rates in the stream network and 2) identify sub-catchments that supply water and organic carbon with high oxygen demand.

2. Methods

2.1. Study site

The study was conducted on the stream network within the 116 km² catchment area that drains into Lake Fil, located in South-West Jutland, Denmark (55°42'N, 8°14'E). The catchment area is mainly used for agriculture (87%), while the remaining land uses include coniferous forest (4%), woodland-shrub (4%), and a mixture of different other uses (5%). All sampling sites received water primarily from agricultural land, while sites closer to the lake included some inland marsh areas. Soil types within the catchment were primarily meltwater sand (67%), clayey till (8%), and freshwater peat (8%).

Lake Fil receives most of its water from the small lake Søvig Sund, which in turn is fed by two streams that drain the catchment area (Fig. 1). Thirteen sites in the catchment were studied, only 11 sites were included in the first sampling. Two of the sites were located in the southern tributary (marked 1S and 2S), while the remaining eleven were located in the northern tributary. Three sites were placed close to each other (3–5), this was the case as the stream split into two tributaries, thereby creating a site in each tributary and one in the downstream stream.

Samples used to test oxygen consumption, and the presence of environmental variables were taken on five occasions selected to ensure analysis of water carried by streams under a variety of weather conditions. Before the first sampling in August 2019, it had been a relatively dry summer period, while the second sampling was done six days later, shortly after a rain event. The third sampling, in September 2019, was done after an extended but gentle rainy period. The final two samplings were done in August 2020, first after a period of low precipitation and then immediately following a heavy precipitation event (ca. 35 mm, Fig. S3). The fifth sample from site 0 was lost.

2.2. Stream discharge

Stream discharge (Q) was measured continuously at each site. Q was calculated as the product of the average cross-sectional channel area and average water velocity. Each site was defined as a 30-m stretch of the stream (with the exception of site 7, which was located at a drainpipe; and stream discharge could not be measured). At the beginning, middle, and end of the 30-m stretch, the depth was measured every 25 cm for the entire width (which ranged from 0.5 m to 4 m). Depth measurements were interpolated linearly, and the mean cross-sectional area was calculated for the three transects. The mean water velocity was measured by injecting a pulse of dissolved NaCl upstream and measuring the time required for 50% of the NaCl to arrive downstream (Allen, 1923).

Water discharge was determined throughout the sampling period, and each site was equipped with a pressure sensor measuring water level (Odyssey, Dataflow Systems, New Zealand) that logged every 10 min

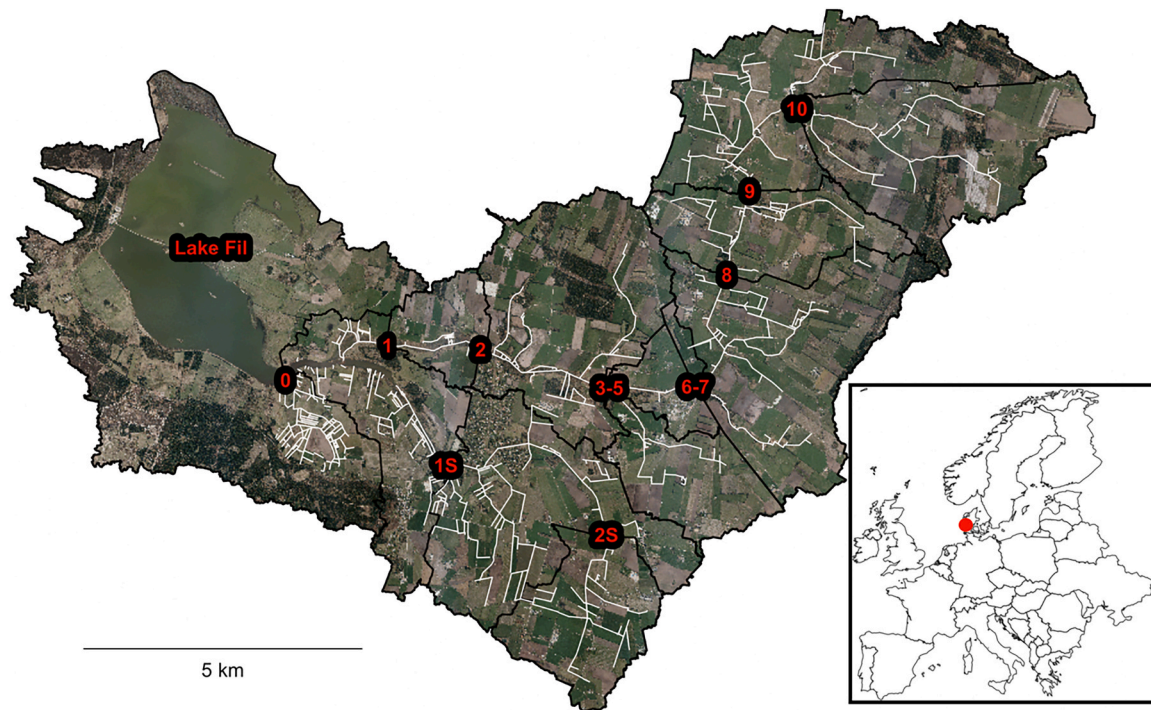


Fig. 1. The catchment area. A northern and southern tributary feeds lake Filso, which is located in the upper-left corner. Red numbers indicate sites examined. Sites 3–5 were located very close to each other, with site 3 closest to the lake and sites 4 and 5 in the northern and southern branches, respectively. Site 7 was a drainpipe outlet just upstream of site 6. White lines indicate the stream network, whereas black lines indicate the sub-catchments. Right corner: Map of Europe showing the location of Lake Fil (red dot). (For interpretation of the references to colour in this figure legend, the reader is referred to the web version of this article.)

from August 2019 to December 2019 and again from April 2020 to October 2020. As a backup, water discharge could be determined by using data from an acoustic doppler (SonTek IQ, Xylem Inc., USA) at the inlet to Lake Fil (site 0), with data from the previous year to determine the relationship of discharge between site 0 and all other sites. The redundancy of being able to determine water flow from the acoustic doppler was fortunate as all pressure sensor data for August 2020 to October 2020 were lost due to a malfunction.

The relationship between Q and water level (H) was determined on four occasions at all sites and described by the Q - H relationship:

$$Q = a \times H^b \quad (1)$$

where Q is a function of H , and a and b are site-specific parameters. Non-linear least-squares models from the stats R package (R Core Team, 2018) were used to determine a and b . Extrapolation of Q was limited to 0.4 and 2.5 times the lowest and highest Q measured, respectively (Bovee et al., 1978). Between the first and second sampling, the site 4 logger disappeared. The discharge at site 4 between first and second sampling period was calculated as the difference between sites 3 and 5 (50 m downstream).

2.3. Oxygen consumption

Water samples rested for at least 3.5 h after sample collection to avoid measurement errors associated with initial oxidation of reduced iron, and at most, 24 h, to avoid errors associated with organic substrate limitation after extended incubation. Within the measuring window, we determined each sample's rate of linear decline by measuring its oxygen concentration continuously at 20.0 °C for a minimum of eight hours in glass incubation bottles (60 mL) equipped with oxygen sensor spots (OXSP5-SUB, Pyroscience, Germany). The temperature in the incubation chamber and oxygen concentration within the incubation bottles were measured every second. Oxygen concentrations were measured by FireStingO2 Logger V2.36 with Firesting O2 Firmware 2.30. To ensure

the reproducibility of the method, replicate samples were measured during the experiment to determine the standard error of the mean on selected samples. Thus, we focused on high accuracy of the oxygen consumption rate of each sample. However, because we had to measure 13 samples within 24 h to avoid errors associated with reduction of oxygen consumption after longer storage, we measured oxygen consumption routinely on only one sample from each stream site but showed that the variability was very low between replicate or triplicate samples from selected stream sites. Oxygen consumption rates were determined based on an average of 33,854 point measurements.

All bottles were kept in a water-filled incubation chamber to avoid temperature fluctuations that could influence oxygen measurements. Constant water temperature (variations below 0.1 °C) was secured by combining a cooling (Hetofrig CB11, Heto-Holten A/S, Denmark) and a heating unit with a high precision regulation unit (Julabo immersion circulation EC 12876, Julabo GmbH, Germany). In the cooling bath, two pumps were used to circulate water in a hose, with parts of the hose submerged in the incubation chamber to keep the temperature stable (Fig. S1).

The discharge-integrated oxygen consumption (DIOC) was calculated by multiplying the oxygen consumption rate by the discharge at the time of sampling. The result is expressed as the oxygen consumption per hour for the water volume passing the site every hour ($\text{g O}_2 \text{ h}^{-1}$). DIOC was interpolated between sites, using inverse-path distance weighting to map oxygen consumption for the entire stream network. Land is understood to be a barrier and was not included during interpolation.

2.4. Environmental variables

A water sample was taken at each site and kept refrigerated (5 °C) or frozen (−18 °C) until analysis. Duplicate subsamples were extracted from the initial sample, which were used for all analyses, with the exception of CDOM and DOM where only one subsample was used.

Analyses of CDOM light absorbance and fluorescence emission spectra of DOM were made on refrigerated samples after 3 days and occasionally longer (up to 14 days). Water samples were filtered through a 0.7 µm GF/F filter (Whatman, UK). CDOM absorbance was measured in a 1 cm cuvette from 239 to 800 nm with 3 nm-increments using a fluorescence spectrometer (Aqualog UV-800-C, Horiba, Japan). Excitation-emission matrices (EEM) of all samples were measured with excitation wavelengths at 5 nm intervals, from 250 to 395 nm, on the same instrument. EEM's were blank-, scatter- and inner filter-effect corrected, using milli-Q water as a blank. All samples were Raman normalized following the procedure by Pucher (2020). PARAFAC modeling followed the procedure described by Murphy et al. (2013), subsequently evaluating the model by a split-half analysis. Corrections, PARAFAC modeling, and split-half analysis were done in MATLAB (The Mathworks Inc., 2020) using the drEEM toolbox version 0.6.0 (Murphy et al., 2013).

PARAFAC component peaks were compared to literature published earlier on the OpenFluor database (Murphy et al., 2014a, 2014b) to characterize the components and identify potential sources.

DOC was measured using a total organic carbon analyzer (Shimadzu TOC-5000) following the methods in Kragh and Søndergaard (2004). To characterize the lability of the DOM, SUVA was calculated by dividing UV-absorbance at 254 nm (m^{-1}) by DOC concentration ($mg\ C\ L^{-1}$) (Weishaar et al., 2003).

Concentrations of total dissolved phosphorus (TDP), total dissolved nitrogen (TDN), ortho-phosphate, nitrate, and ammonium were measured on all samples using standard methods on an autoanalyzer (AA3HRAutoAnalyzer, SEAL) as described in Kristensen et al. (2018) and Kragh and Søndergaard (2004).

2.5. Statistical analyses

To identify variables that influence the stream water oxygen consumption rate, we fitted linear mixed effect models (LMM) with oxygen consumption rate as the dependent variable and PARAFAC component loadings, SUVA, nutrient concentrations, land use (European Environment Agency, 2019), and soil type (National Geological Survey for Denmark and Greenland, 2015) as predictors. LMM with 'site' as a random intercept was used to account for the repeated samplings because observations within sites are likely to be more similar than between sites and thus not independent. Furthermore, LMM handles observations, including missing data (Cnaan et al., 1997; Laird and Ware, 1982).

Land use and soil type both consisted of 12 highly correlated categories. Principal component analysis (PCA) was performed on each group to avoid inter-correlated variables. All principal components (PC) explaining 20% or more of the variance in the data were used for the LMM. Prior to modeling, all independent variables were scaled and examined for inter-correlation using Spearman-rank correlation. Variables with a Spearman ρ between -0.39 and 0.39 were assumed to be non-correlated. If two variables had higher correlation coefficients, only one of the variables was kept, based on the highest correlation coefficient with oxygen consumption rate or previous significant results.

LMM model selection was performed using a backward elimination approach until the relationship between oxygen consumption rate and independent variables were significant ($p < 0.05$) or showed a tendency ($p < 0.1$). Marginal and conditional R^2 coefficients were also determined (Nakagawa and Schielzeth, 2013). The marginal R^2 concerns the variance explained by fixed effects only, whereas the conditional R^2 concerns the variance explained by fixed and random effects.

To visualize the differences between sites and samplings, we used PCA and t-SNE (t-distributed stochastic neighbor embedding). The t-SNE is a visualization method that models high-dimensional data into a lower dimensional space where similar observations are located closer to each other. For the t-SNE method, we used the *Rtsne* R-package (Krijthe, 2015), with the perplexity parameter set to 10.

All data processing was made in R (R Core Team, 2018), using the

Tidyverse package (Wickham et al., 2019). We used the *sf* (Pebesma, 2018) and *raster* (Hijmans, 2019) for spatial data, and the *ipdw* (Stachek, 2019) package to interpolate DIOC. The *lme4* (Bates et al., 2015) and *car* packages (Fox and Weisberg, 2019) were used for modeling, while the pseudo- R^2 was determined using the *MuMIn* package (Bartoń, 2018).

3. Results

3.1. Stream discharge

Discharge between sites showed similar temporal patterns throughout the catchment, characterized by peaks occurring earlier at upstream sites further away from the lake but eventually accumulating closer to the lake (Fig. S2). During a rain event on 29 September 2019, an immediate flow peak was present at the upstream site 10; the flow peaked 35.6 h later at site 1, located 14.4 km downstream. The delay corresponds to an average water velocity through the catchment of $0.40\ km\ h^{-1}$ or $11\ cm\ s^{-1}$. Thus, it is possible to catch a peak flow event at an upstream site during a sampling campaign and miss it downstream or vice versa.

Discharge was expected to be highest at site 0, the most downstream site, but during some periods, higher discharge was recorded at nearby upstream sites. The error is probably due to the estimation of discharge (Q) from the Q-H relationship (e.g., too few measurements during high-discharge periods, or unrecorded water running at unknown velocity underneath the banks or through dense vegetation).

3.2. Oxygen consumption

Oxygen consumption rates exhibited high variation among sites, although mean values for all sites showed little variation, except for the fifth sampling. The second sampling at site 9 showed the lowest oxygen consumption rate overall ($11\ \mu g\ O_2\ L^{-1}\ h^{-1}$), while the last sampling at site 2 showed the highest rate overall ($339\ \mu g\ O_2\ L^{-1}\ h^{-1}$) (Fig. 2). The second sampling campaign in 2019 showed the lowest mean oxygen consumption rate and variation (mean: 26.5 and SD: $8.4\ \mu g\ O_2\ L^{-1}\ h^{-1}$), while the last sampling campaign in 2020 showed the highest mean values and variation between sites (mean: $105\ \mu g\ O_2\ L^{-1}\ h^{-1}$, SD: $97.4\ \mu g\ O_2\ L^{-1}\ h^{-1}$). Oxygen consumption rates varied 19-fold between sampling dates at site 2, but only 2–7-fold at all other sites.

Two replicate and two triplicate measurements of oxygen consumption rates showed a low standard error of the mean (SEM) ranging from 2 to 15% of the mean.

DIOC was highest at stream sites closest to the lake inlet and lowest at upstream sites of low discharge (Fig. 3). The first four sampling events showed a limited variation of mean DIOC across sites (28.2 – $59.7\ g\ O_2\ h^{-1}$), while the fifth sampling in August 2020 showed the highest average DIOC ($215\ g\ O_2\ h^{-1}$) due to vast increases at sites 2, 4, and 7.

3.3. Environmental variables

PARAFAC analysis of the DOM revealed five distinct components, when compared with earlier published excitation and emission spectra data (Fig. S4, Table 1). Fluorescence properties of components 1–4 were similar to earlier described humic-like components, while component 5 showed properties similar to tryptophan. Fluorescence properties of components 1 and 3 have previously been shown to indicate terrestrial derived DOM, while component 2 indicates wastewater or animal waste, and component 4 indicates DOM exported from agricultural catchments. Components 2, 3, and 4 were inter-correlated, which was expected as they all originate from agricultural sources.

PARAFAC component loadings varied between both samplings and sites. Site 2S showed high components loadings in all samplings, with especially high loadings of components 2, 3, and 4 (Fig. 4). High loadings of components 2, 3, and 4 were expected as the entire sub-catchment of site 2S consists of farmland. However, site 5 had low

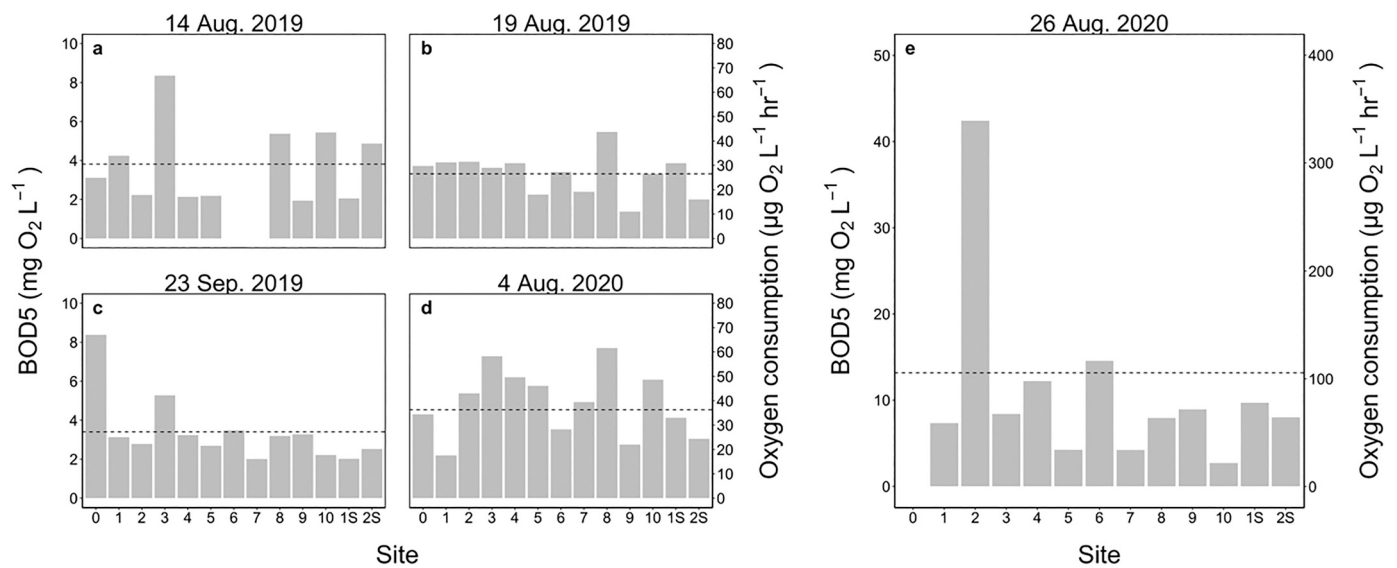


Fig. 2. Oxygen consumption rate at each site on five dates. Dotted lines indicate mean values for each sampling date. Panel a indicates the first sampling, which was done on August 14. Panel b indicates the second sampling, which was done on August 19, and so forth. Sites are ordered according to the North and South stream section (1S + 2S) and distance from the lake inlet (0 being closest, 10 being furthest away). Note the difference in the y-axis on the 26 Aug. 2020.

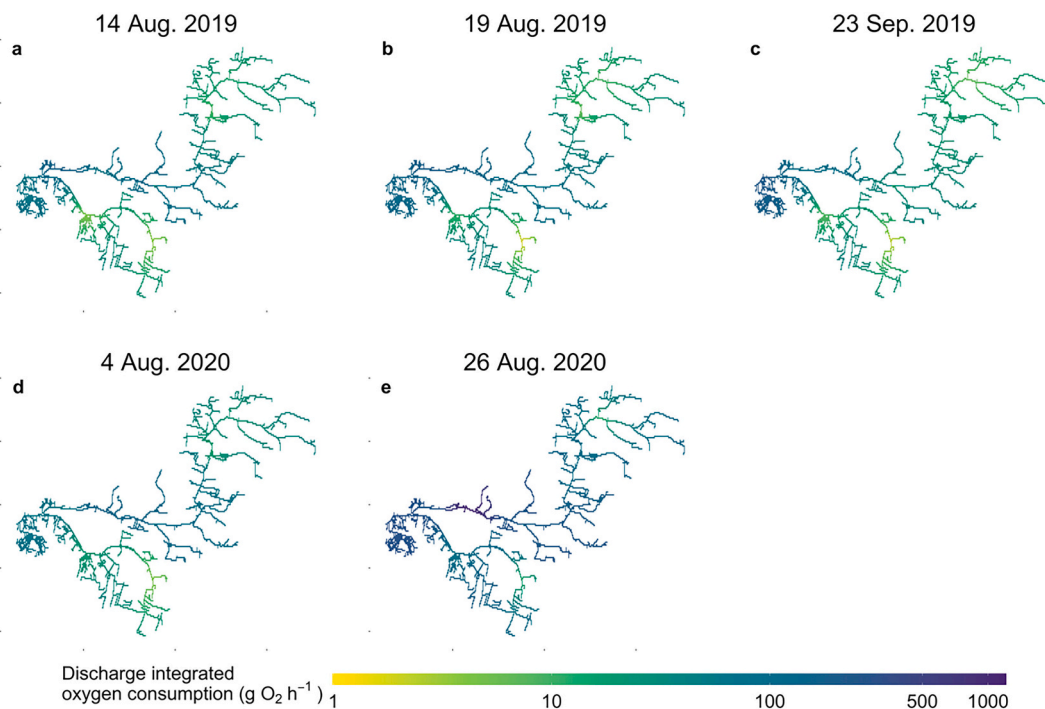


Fig. 3. Discharge-integrated oxygen consumption for the entire stream network ($\text{g O}_2 \text{h}^{-1}$). Panel a indicates the first sampling, which was done on August 14. Panel b indicates the second sampling, which was done on August 19, and so forth.

component loadings throughout the samplings, despite having land use resembling site 2S. The uppermost site 10, receiving water from primarily agricultural catchment (90%), showed low overall loadings. Overall, agricultural land use was dominant within all catchments, causing less variation among components.

DOC varied among sampling campaigns with lower concentrations in the first and fourth sampling (mean: 3.1 and 3.7 mg C L^{-1} , respectively) and higher concentrations in the second, third, and fifth sampling (5.1, 4.7, and 7 mg C L^{-1} , respectively; Fig. 5). Sites 6 and 7 showed the highest DOC concentrations, with a slight decrease at sites located further upstream or downstream. The southern sites (1S and 2S) in the

stream network usually had higher DOC concentrations than the northern sites.

Average specific UV absorbance at 254 nm (SUVA) showed profound variation among sites. Values tended to increase from the first to the fifth sampling campaign, except for the last sampling in August 2020 (Fig. 5). Average SUVA among sites increased slightly from the first to the third sampling in 2019 (mean: 3.1 to 3.7 $\text{L mg}^{-1} \text{C m}^{-1}$, respectively), while SUVA peaked in the fourth sampling (mean: 4.4 $\text{L mg}^{-1} \text{C m}^{-1}$, early August 2020) and decreased in the fifth sampling (mean: 3.8 $\text{L mg}^{-1} \text{C m}^{-1}$, late August 2020). The decrease in SUVA in the fifth sampling was concurrent with the peak flow and the high increase of DOC

Table 1

Excitation and emission peaks of components 1–5 and description of sources and properties from (Murphy et al., 2014a; Stedmon and Markager, 2005).

Component	Excitation	Emission	Description
1	360	452	Fulvic acid fluorophore group. Present in all environments. Origin: Terrestrial/autochthonous.
2	315	396	Humic fluorophore, dominating the fluorescence of wastewater DOM. Correlated to DOM exported from agricultural catchments, possibly due to the spreading of animal waste on fields as fertilizer. Origin: Anthropogenic.
3	405	507	Derived from photochemical degradation of terrestrial organic matter. Origin: Terrestrial.
4	<250	447	Humic fluorophore group. Dominating the DOM exported from the natural catchments during the warmer months of the year. Exported from agricultural catchments. Absent in wastewater. Origin: Terrestrial.
5	280	337	Tryptophan-like fluorescence. Fluorescence peak almost identical to free tryptophan. Derived from autochthonous processes. Correlated to terrestrial fluorescent material in forested catchments. Origin: Autochthonous

concentrations.

Stream sites could be plotted in two dimensions based on the measured environmental parameters, using two different methods for dimensionality reduction. The first two components of a conventional PCA explained 63% of the variation (Table S1, Table S2). Furthermore, general clustering for the samplings and some separation between the sites in the southern (S1 and S2) and northern part of the stream network (Fig. 6 A) were noticeable. Visualizing the same data using t-SNE showed much better separation between samplings, and especially the fifth sampling appeared very different from the previous four. The first and fourth samplings appeared very similar, even more than the first and second samplings, which were only five days apart (Fig. 6 B).

Nutrient levels in the stream network were generally high. TDN, dominated by nitrate, increased from late summer to early autumn. Ammonium and TDP did not show any distinct patterns. TDN and nitrate showed a pattern towards higher concentrations over time (Table 2).

3.4. Drivers of oxygen consumption rate

In order to include land use and soil type as possible environmental predictors of oxygen consumption rates, principal component analyses were conducted, resulting in the identification of 1 principal component (PC) for land use and 2 PCs for soil type. Due to inter-correlation, only 8 predictor variables were used in the model: land use PC1, soil type PC1, PC2, tryptophan loadings (PARAFAC component 5), ammonium, SUVA, and TDP concentrations. Following model selection, two predictors of

oxygen consumption rate, namely tryptophan loadings and SUVA showed significant relationships (t-value = 8.21, $p < 0.001$, t-value = -2.2, $p = 0.03$, respectively) and ammonium a distinct tendency (t-value = 1.83, $p = 0.074$). Ammonium concentrations and tryptophan loadings showed positive relationships with oxygen consumption rate (estimates: 7.7 and 31.3 $\mu\text{g O}_2 \text{L}^{-1} \text{h}^{-1}$, respectively), presumably reflecting increasing lability of organic matter, while SUVA showed a negative relationship (estimate: -8.6 $\mu\text{g O}_2 \text{L}^{-1} \text{h}^{-1}$) reflecting increasing aromaticity and lower lability of organic matter. The LMM for the three predictor variables had a marginal and conditional pseudo- R^2 of 58% and 65%, respectively. Thus, tryptophan loading, SUVA, and ammonium concentration accounted for 58% of the variation in oxygen consumption rate, while 7% of the variation was accounted for by the site differences (random effect).

4. Discussion

4.1. Drivers of stream oxygen consumption

We identified tryptophan loading (PARAFAC component 5), ammonium concentration, and SUVA as the three significant variables that accounted for two-thirds of the spatial and temporal variability of oxygen consumption rates among the 13 sites and five samplings in the stream network. PARAFAC component 5 has been interpreted as tryptophan loading and a positive indicator of the DOC lability (Hudson et al., 2008; Khamis et al., 2015), while SUVA, in contrast, is a measure

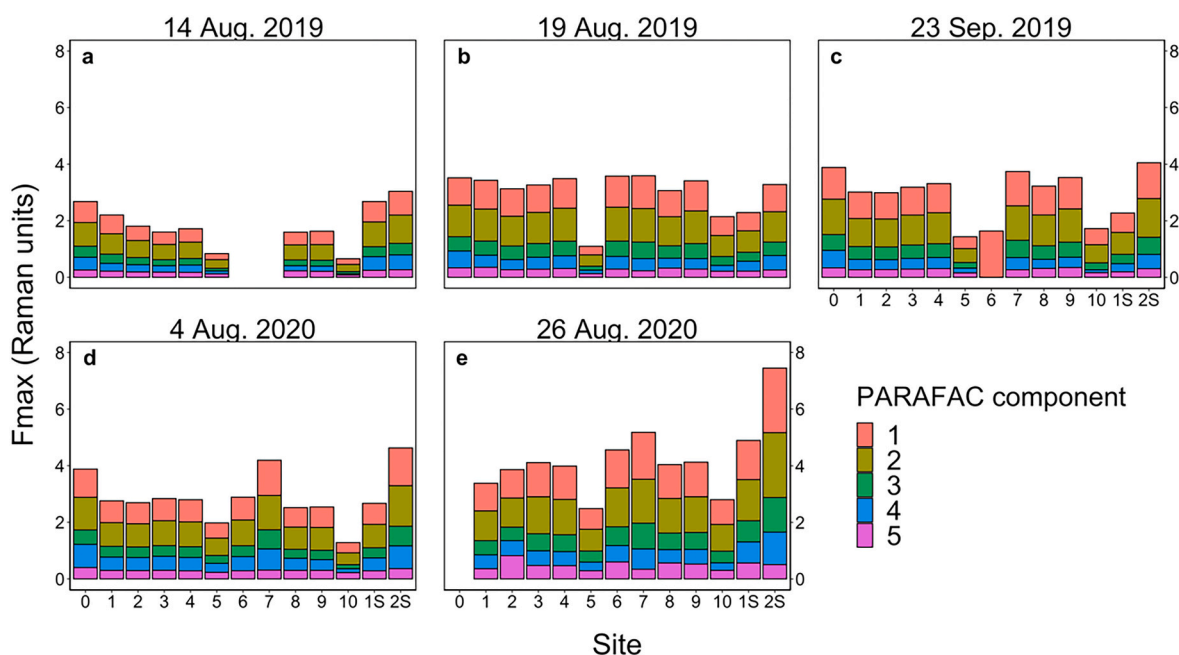


Fig. 4. PARAFAC component loadings at each site in Raman Units (RU). Sites 6 and 7 were not included in the first sampling. Panel a indicates the first sampling, which was done on August 14. Panel b indicates the second sampling, which was done on August 19, and so forth. Sites are ordered according to the North and South stream section (1S + 2S) and distance from the lake inlet (0 being closest, 10 being furthest away).

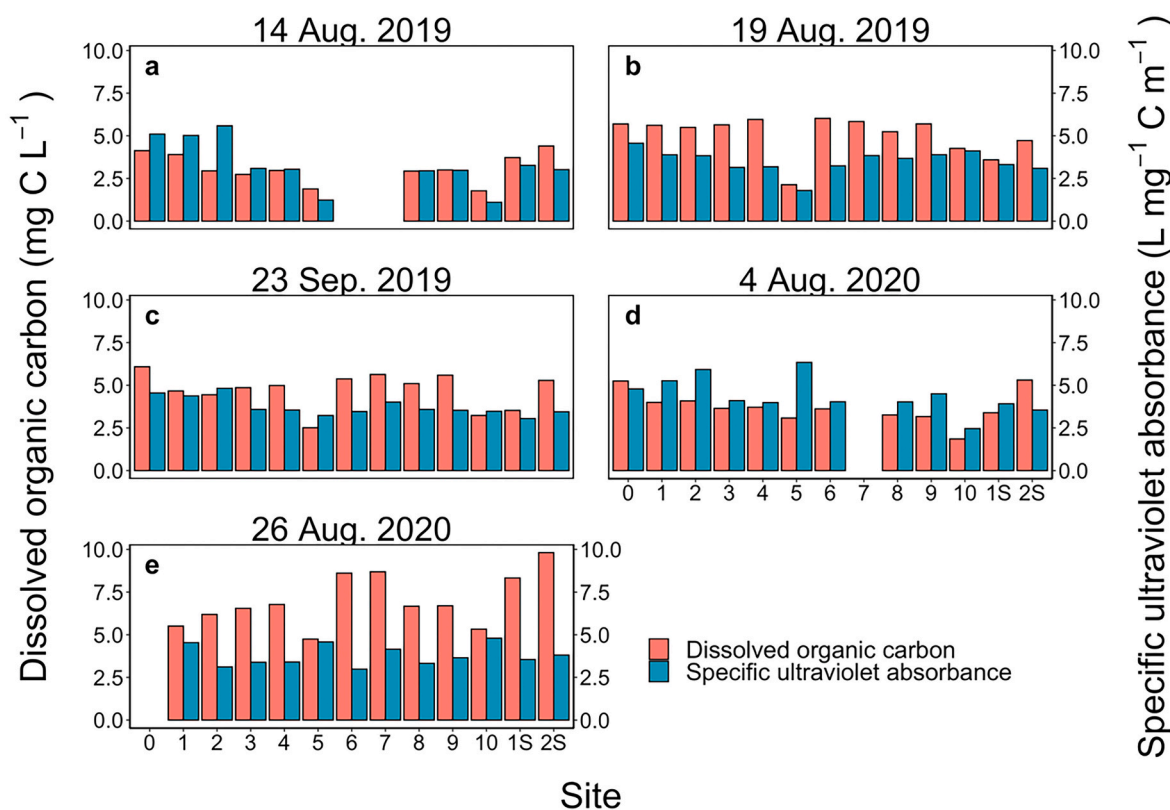


Fig. 5. Dissolved organic carbon (DOC, mg C L^{-1}) and specific UV-absorbance at 254 nm (SUVA, $\text{L mg}^{-1} \text{C m}^{-1}$) at each site. The red bar indicates DOC (left y-axis), and the blue bar indicates SUVA (right y-axis). Panel a indicates the first sampling, which was done on August 14. Panel b indicates the second sampling, which was done on August 19, and so forth. Sites are ordered according to the North and South stream section (1S + 2S) and distance from the lake inlet (1 being closest, 10 being furthest away). (For interpretation of the references to colour in this figure legend, the reader is referred to the web version of this article.)

of DOC aromaticity. Thus, lower DOC lability is expected with increasing SUVA, and it was negatively related to oxygen consumption rate in accordance with [Figueroa-Nieves et al. \(2014\)](#). High ammonium concentration is anticipated in water with high microbial activity, and a positive coupling to oxygen consumption rate is expected ([van Kessel et al., 2015](#)), as we indeed observed.

High tryptophan loadings have been found in sewage water ([Chen et al., 2003](#); [Reynolds, 2002](#); [Reynolds and Ahmad, 1997](#)) and water from flooded pastures ([Baker, 2002](#)), thus making it possible to trace point sources of pollution in natural waters. Sites 2, 8, and 9 in our stream network showed particularly high tryptophan loadings, indicating point sources of labile organic matter at those sites that could be attributed to the high proportion of agricultural land use within the catchments. Some sites experienced decreased tryptophan loadings through time, most likely due to depletion of the terrestrial organic matter later in summer and early autumn as well as dilution by higher water discharges leading to lower oxygen consumption rates. In contrast, tryptophan loadings and oxygen consumption rates were particularly high during the fifth sampling in August 2020 during a flow peak event following a dry period. The high tryptophan loadings and oxygen consumption rates suggest a profound washout from the soils of labile DOC that had accumulated during the preceding warm, dry period. A mechanism that has previously been proposed ([Moelund et al., 2018](#)) and is in accordance with the high input of labile DOC to Lake Fil during the high flow event following an extended period of drought in the summer of 2018 ([Kragh et al., 2020](#)).

The oxygen consumption rate was positively related to ammonium concentration. The relationship may reflect an indirect positive coupling to overall microbial activity ([van Kessel et al., 2015](#)) and a direct coupling due to the oxygen demanding nitrification transfer process of ammonium

to nitrate. The stream inlet to Lake Fil has a mean ammonium concentration of 0.3 mg N L^{-1} , which requires $1.38 \text{ mg O}_2 \text{ L}^{-1}$ for conversion to nitrate, or about 13.8% of a typical oxygen concentration of $10 \text{ mg O}_2 \text{ L}^{-1}$. Most of the area within the lake catchment is agricultural land that is drained and fertilized and releases high amounts of ammonium and nitrate into the stream network. As already emphasized, high nutrient concentrations are expected to increase the microbial biomass and associated oxygen consumption rates with nitrifying bacteria likely contributing to the oxygen demand ([Fierer et al., 2005](#); [Meyer and Johnson, 1983](#); [Peters et al., 1987](#); [White et al., 1991](#)). The nitrate produced will then serve as an alternative electron acceptor to oxygen in anaerobic organic degradation by denitrification in the lake ([Knowles, 1982](#)).

SUVA is positively correlated with DOC aromaticity ([Weishaar et al., 2003](#)). Microbial degradation of aromatic organic compounds is slow due to the stability of the aromatic rings, causing lower degradation rates compared to organic compounds of low aromaticity ([Fuchs et al., 2011](#)). Using SUVA as a proxy for DOC aromaticity, we found a negative relationship with oxygen consumption rates. SUVA measurements could potentially be used as an indicator of pollution sources: areas with low SUVA (i.e., low DOC aromaticity) could be the result of extensive fertilizer application, organic spills from farms, and wastewater outlets of low DOC aromaticity, however these possible relationships were not tested.

Knowing the main predictors of oxygen consumption rates in an agricultural stream network can assist managers in obtaining higher ecological quality by identifying potentially problematic sub-catchments that deliver water with high oxygen demand. Problematic sub-catchments could be dealt with by managing water flow close to hotspots.

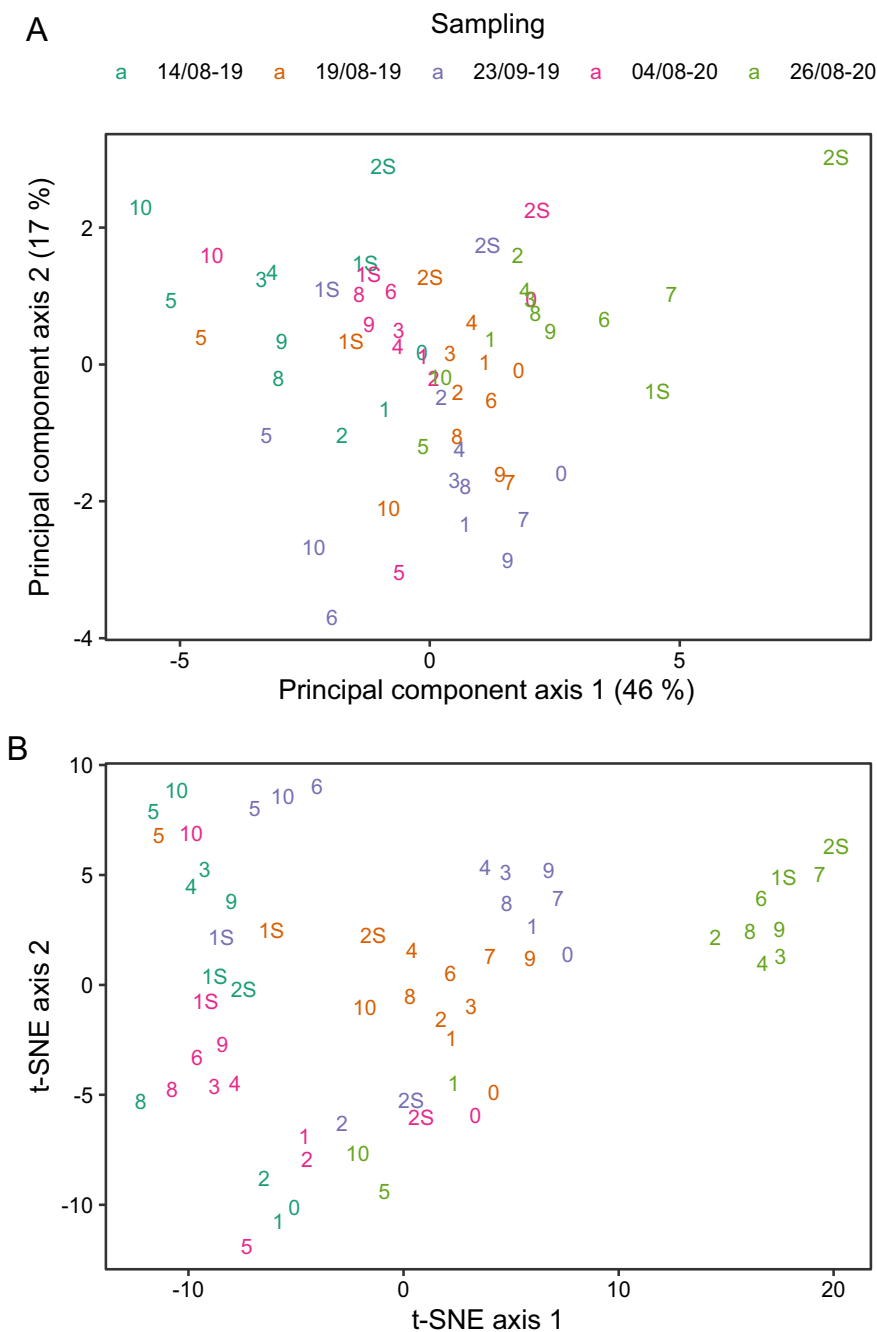


Fig. 6. Stream sites are colored by sampling time and visualized using PCA (A) and two-dimensional t-SNE (B). Sites are modelled into a low-dimensional space based on the measured environmental variables.

Table 2

Nutrient concentrations (mean ± SD, unit: $\mu\text{g L}^{-1}$) on the five sampling occasions.

Sampling date	TDN-N	NO ₃ -N	NH ₄ -N	TDP-P	PO ₄ -P
14 August 2019	956 ± 395	423 ± 200	227 ± 367	21.2 ± 9.7	4.0 ± 5.0
19 August 2019	1296 ± 380	834 ± 361	152 ± 84.3	39.7 ± 15	7.6 ± 4.4
23 September 2019	1823 ± 566	1425 ± 546	183 ± 102	26.7 ± 7.0	9.0 ± 4.1
4 August 2020	1226 ± 424	631 ± 103	183 ± 126	18.4 ± 9.4	6.4 ± 4.7
26 August 2020	1759 ± 583	832 ± 279	280 ± 152	18.8 ± 6.4	4.6 ± 2.9

4.2. Implications for lake oxygen conditions

In early August 2018, the southern part of Lake Fil suffered a massive fish kill after a long period of heat and drought followed by a heavy precipitation event that caused a profound inlet of organic-rich stream water. The lake experienced a sudden 2.3-fold increase in respiration, from $0.35 \text{ g O}_2 \text{ m}^{-3} \text{ h}^{-1}$ to $0.82 \text{ g O}_2 \text{ m}^{-3} \text{ h}^{-1}$, eliciting total anoxia in the water column (Kragh et al., 2020).

In our study, the highest absolute oxygen consumption (DIOC) carried with the water flow in the stream was observed in the fifth sampling; sites 1 and 1S summed to $0.28 \text{ kg O}_2 \text{ h}^{-1}$. However, substituting site 1 for site 2, thus summing sites 2 and 1S, absolute oxygen consumption was $1.09 \text{ kg O}_2 \text{ h}^{-1}$. Apparently, we hit the peak inflow during sampling at site 2 but missed it at site 1. Nevertheless, the high oxygen consumption rate measured in the stream on the fifth sampling was not noticeable in the continuous oxygen measurements in the lake at the site closest to the inlet (data not shown, sensor location in Kragh et al. (2020) Fig. S5). Thus, although oxygen consumption in the stream water was high, it did not pose a threat to oxygen conditions in the lake in contrast to the situation in early August 2018. The difference could be attributed to a much higher input of DOC and CDOM in early August 2018, resulting in very high DOC concentrations and higher CDOM light absorbance in the lake compared with late August 2020. Moreover, water temperature in Lake Fil was particularly high prior to and during the early August 2018 event ($25 \text{ }^\circ\text{C}$), resulting in an increased oxygen consumption rate, whereas in-lake water temperature in late August 2020 was much lower ($15 \text{ }^\circ\text{C}$, Fig. S5), thereby reducing the oxygen consumption rate relative to our measurements at $20 \text{ }^\circ\text{C}$. Overall, the stronger increase of DOC and CDOM in early August 2018 indicates a more extensive stream input and a lower dilution within the lake which had a much-reduced water level due to the extensive drought preceding the storm flow event. In addition, DOC input in early August 2018 was assumed to be highly labile as the concentration decreased rapidly in the lake over a few days (Kragh et al., 2020). DOC flushed into the stream under normal, stable flow conditions and moderate soil temperatures are presumably less labile and may have undergone substantial degradation already in the soil matrix (Madsen-Østerbye et al., 2018; Webster and Benfield, 1986). The hypothesis is further supported by the relatively high and increasing aromaticity of DOC throughout the samplings from August to October 2019, as reflected by high and increasing SUVA (Weishaar et al., 2003). The pattern was not the same from early to later in August 2020, perhaps due to a different time course of precipitation and flushing of soil DOC into the stream.

4.3. Challenges to identifying hotspots of oxygen consumption

In large catchments such as Lake Fil's, it is hard to identify particularly high or problematic organic sources. Furthermore, identification of organic sources can be difficult due to heavy drainage of the catchment, which may lead to extensive flushing of water through unmapped or veiled drain pipes. While effluent water from the most upstream sites can be identified as emerging from a specific sub-catchment, sites located further downstream receive water from many sub-catchments. Thus, further research is needed at a finer spatial resolution to trace problematic point sources by specifically measuring those environmental variables identified in this study that contribute to high oxygen consumption rates.

The ability to determine the chemical composition and oxygen consumption rate of water and thereby tracing it to individual agricultural fields, grasslands, cities, or forests would make it easier to determine sub-catchments that pose a threat to downstream systems. Using PCA and t-SNE techniques, it was possible to achieve good separation of the different samplings based on measured water chemical variables despite the very homogenous catchment of Lake Fil, with agriculture claiming more than 87%. However, the differences in chemical composition were generally (except for the fifth sampling) not reflected

in oxygen consumption rates showing small differences.

The two sites in the southern network, S1 and S2, were different from the rest of the sites on most occasions. However, discriminating between sites in the northern stream network was more difficult, although some sites, e.g., site 5, appeared well clustered in three dimensions. Thus, these statistical tools appear promising for future work on separate stream sites based on multiple observations of water chemistry. The separation of environmental variables is expected to improve when sampling sub-catchments with contrasting land use. Including neighboring catchments with similar soil types but different land use (i.e., nature, towns, and particularly intensive agriculture) may generate stronger gradients and better predictions of which environmental variables account for the differences in oxygen consumption rates.

Our sampling was conducted at distinctive weather scenarios with the hope of reproducing extended summer drought followed by heavy rain, as in August 2018. However, our study period did not include comparable long and warm drought periods followed by heavy rain. Nonetheless, the importance of weather conditions is reflected in the extensive differences between the fifth sampling and the four earlier samplings. We believe the differences are even greater after events with higher precipitation, following an extended summer drought, and after a concentrated spreading of liquid manure. In retrospect, to determine the full effect of weather conditions on stream oxygen consumption rate, it would be preferable to apply a research method that included continuous measurements of water flow, oxygen consumption rate, tryptophan, and SUVA at several sites within the stream network.

4.4. Future directions

This study has helped to identify problematic sites of high oxygen consumption rates of effluent water within Lake Fil's catchment, with the model explaining two-thirds of the variation in oxygen consumption rates. Being able to determine factors influencing oxygen consumption rates and quantifying these factors throughout the stream network, have created a useful tool for managers in determining areas that should be prioritized for restoration projects. Better restoration projects could result from easier determination of sources that contributes the most to high oxygen consumption rates.

Climate change poses a new threat to the freshwater environment due to more frequent periods of extended drought and heavy precipitation, like the event in early August 2018, causing total anoxia and massive fish kill in Lake Fil. It was indeed a rare event, as no oxygen measurements during the earlier six years had revealed periods of total lake anoxia (Kragh et al., 2020). However, if no action is taken to mitigate the environmental threats, these anoxic events and their associated fish kills are likely to occur more often in the future due to warmer and more dramatic weather. To improve understanding of events like that of August 2018, stronger measurement strategies could be implemented, including continuous on-site measurements of tryptophan and water flow, which showed to be the main contributors to increased oxygen consumption rates. Thereby, it should be possible to continuously quantify mass balances of oxygen demand, and losses or gains between sites. Additionally, on-site measurements of oxygen consumption rates would be favorable, thereby getting a better understanding of weather and seasonal effects on oxygen consumption rates.

Once problematic sub-catchments or specific point sources have been identified, it will be possible to reduce their influence. For example, some low-lying areas under intensive cultivation may turn out to be problematic due to extensive flooding and the export of much labile organic matter following heavy rain (Moeslund et al., 2018). Moreover, low-lying areas, typically high in soil organic carbon, are also extensive emitters of greenhouse gases (Tiemeyer et al., 2020). Handling ascertained problematic sources in the farmland could be dealt with by biogas facilities treating water with particularly high concentrations of nutrients and organic carbon, which is in turn utilized in the formation of methane (CH_4) used for heating or formation of electricity (Gür,

2016). Thereby, both nutrients and organic carbon loading are reduced in the effluent water (Xu et al., 2015). Other potential solutions may involve turning areas close to the stream into wetlands with benefits for both climate and freshwater biodiversity. New freshwater habitats would reduce nutrients and carbon before they enter the stream (Verhoeven and Meuleman, 1999), while decreasing the pulse input of water and the risk of anoxia following extreme rain events (Aceman and Holden, 2013).

Author statement

All authors contributed to the conceptualization of the project, with Theis Kragh (TK) and Kaj Sand-Jensen (KSJ) developing the idea of this project. Methodology was conducted by all authors. Formal analysis was performed by Jonas Stage Sjø (JSS) and Kenneth Thorø Martinsen (KTM), while investigation was done by JSS, TK and KTM. Writing the original draft was done by JSS, while reviewing and editing was done by all authors. Visualization was done by JSS and KTM. Funding acquisition was done by KSJ and TK.

Declaration of Competing Interest

The authors declare that they have no known competing financial interests or personal relationships that could have appeared to influence the work reported in this paper.

Acknowledgments

We thank the Aage V. Jensen Foundation for grants to TK, KSJ, and KTM and accommodation during field visits. We thank Colin Stedmon and Urban Wunsch for assistance and use of equipment. Furthermore, we thank David Sturligross for proofreading the manuscript.

Appendix A. Supplementary data

Supplementary data to this article can be found online at <https://doi.org/10.1016/j.ecoleng.2021.106516>.

References

- Aceman, M., Holden, J., 2013. How wetlands affect floods. *Wetlands* 33 (5), 773–786.
- Ahmad, S.R., Reynolds, D.M., 1999. Monitoring of water quality using fluorescence technique: Prospect of on-line process control. *Water Res.* 33 (9), 2069–2074. [https://doi.org/10.1016/S0043-1354\(98\)00435-7](https://doi.org/10.1016/S0043-1354(98)00435-7).
- Allan, J.D., Castillo, M.M., 2007. *Stream Ecology: Structure and Function of Running Waters*. Springer Science & Business Media.
- Allen, C.M., 1923. The salt velocity method of water measurement. *Trans. Am. Soc. Mech. Eng.* 45, 285.
- Baker, A., 2002. Fluorescence properties of some farm wastes: implications for water quality monitoring. *Water Res.* 36 (1), 189–195.
- Baker, A., Curry, M., 2004. Fluorescence of leachates from three contrasting landfills. *Water Res.* 38 (10), 2605–2613. <https://doi.org/10.1016/j.watres.2004.02.027>.
- Baker, A., Inverarity, R., 2004. Protein-like fluorescence intensity as a possible tool for determining river water quality. *Hydrol. Process.* 18 (15), 2927–2945. <https://doi.org/10.1002/hyp.5597>.
- Bartoň, K., 2018. MuMIn: Multi-model Inference (Version R package Version 1.42.1). Retrieved from. <https://CRAN.R-project.org/package=MuMIn>.
- Bates, D., Maechler, M., Bolker, B., Walker, S., 2015. Fitting linear mixed-effects models using lme4. *J. Stat. Softw.* 67 (1), 1–48.
- Biggs, J., Von Fumetti, S., Kelly-Quinn, M., 2017. The importance of small waterbodies for biodiversity and ecosystem services: implications for policy makers. *Hydrobiologia* 793 (1), 3–39.
- Bovee, K.D., Milhous, R.T., Turow, J., 1978. *Hydraulic Simulation in Instream Flow Studies: Theory and Techniques*. Department of the Interior, Fish and Wildlife Service, Office of Biological.
- Brookes, A., 1987. The distribution and management of channelized streams in Denmark. *Regul. Rivers Res. Manag.* 1 (1), 3–16. <https://doi.org/10.1002/rrr.3450010103>.
- Chen, W., Westerhoff, P., Leenheer, J.A., Booksh, K., 2003. Fluorescence excitation–emission matrix regional integration to quantify spectra for dissolved organic matter. *Environ. Sci. Technol.* 37 (24), 5701–5710.
- Cnaan, A., Laird, N.M., Slator, P., 1997. Using the general linear mixed model to analyse unbalanced repeated measures and longitudinal data. *Stat. Med.* 16 (20), 2349–2380.

- Comber, S.D.W., Gardner, M.J., Gunn, A.M., 1996. Measurement of absorbance and fluorescence as potential alternatives to BOD. *Environ. Technol.* 17 (7), 771–776. <https://doi.org/10.1080/09593331708616444>.
- Dahl, T.E., 1990. *Wetlands Losses in the United States, 1780's to 1980's*. US Department of the Interior, Fish and Wildlife Service.
- Dahl, T.E., 2011. *Status and Trends of Wetlands in the Conterminous United States 2004 to 2009*. US Department of the Interior, US Fish and Wildlife Service, Fisheries and Habitat Conservation.
- Dudgeon, D., Arthington, A.H., Gessner, M.O., Kawabata, Z.I., Knowler, D.J., Leveque, C., Naiman, R.J., Prieur-Richard, A.H., Soto, D., Stiassny, M.L.J., Sullivan, C.A., 2006. Freshwater biodiversity: importance, threats, status and conservation challenges. *Biol. Rev.* 81 (2), 163–182. <https://doi.org/10.1017/S1464793105006950>.
- Elliott, J.M., 1994. *Quantitative Ecology and the Brown Trout*. Taylor & Francis.
- European Environment Agency, 2019. *Corine Land Cover (CLC) 2018, Version 20*. Retrieved from: <https://land.copernicus.eu/pan-european/corine-land-cover/clc2018>.
- Ferreira, V., Castagnyrol, B., Koricheva, J., Gulis, V., Chauvet, E., Graça, M.A.S., 2015. A meta-analysis of the effects of nutrient enrichment on litter decomposition in streams. *Biol. Rev.* 90 (3), 669–688. <https://doi.org/10.1111/brv.12125>.
- Fierer, N., Craine, J.M., McLaughlan, K., Schimel, J.P., 2005. Litter quality and the temperature sensitivity of decomposition. *Ecology* 86 (2), 320–326. <https://doi.org/10.1890/04-1254>.
- Figueroa-Nieves, D., McDowell, W.H., Potter, J.D., Martínez, G., Ortiz-Zayas, J.R., 2014. Effects of sewage effluents on water quality in tropical streams. *J. Environ. Qual.* 43 (6), 2053–2063. <https://doi.org/10.2134/jeq2014.03.0139>.
- Fox, J., Weisberg, S., 2019. *An {R} Companion to Applied Regression*, 3 ed. Sage, Thousand Oaks CA.
- Fuchs, G., Boll, M., Heider, J., 2011. Microbial degradation of aromatic compounds — from one strategy to four. *Nat. Rev. Microbiol.* 9 (11), 803–816. <https://doi.org/10.1038/nrmicro2652>.
- Gür, T.M., 2016. Comprehensive review of methane conversion in solid oxide fuel cells: prospects for efficient electricity generation from natural gas. *Prog. Energy Combust. Sci.* 54, 1–64. <https://doi.org/10.1016/j.pecs.2015.10.004>.
- Hansen, K., 2008. *The Lost Land - the Great Tale about the Power over the Danish Landscape (in Danish)*. Kbh: Gad.
- Hijmans, R.J., 2019. *Raster: Geographic Data Analysis and Modeling*.
- Hopkinson Jr., C.S., Vallino, J.J., Nolin, A., 2002. Decomposition of dissolved organic matter from the continental margin. *Deep-Sea Res. II Top. Stud. Oceanogr.* 49 (20), 4461–4478.
- Hudson, N., Baker, A., Ward, D., Reynolds, D.M., Brunsdon, C., Carliell-Marquet, C., Browning, S., 2008. Can fluorescence spectrometry be used as a surrogate for the Biochemical Oxygen demand (BOD) test in water quality assessment? An example from South West England. *Sci. Total Environ.* 391 (1), 149–158. <https://doi.org/10.1016/j.scitotenv.2007.10.054>.
- Iversen, T.M., Thorup, J., Skriver, J., 1982. Inputs and transformation of allochthonous particulate organic matter in a headwater stream. *Ecography* 5 (1), 10–19.
- Johnson, F.H., Eyring, H., Stover, B.J., 1974. *New York: John Wiley And Sons*.
- van Kessel, M.A.H.J., Speth, D.R., Albertsen, M., Nielsen, P.H., Op den Camp, H.J.M., Kartal, B., Jetten, M.S.M., Lückler, S., 2015. Complete nitrification by a single microorganism. *Nature* 528 (7583), 555–559. <https://doi.org/10.1038/nature16459>.
- Khamis, K., Sorensen, J., Bradley, C., Hannah, D., Lapworth, D., Stevens, R., 2015. In situ tryptophan-like fluorometers: assessing turbidity and temperature effects for freshwater applications. *Environ Sci Process Impacts* 17 (4), 740–752.
- Knowles, R., 1982. Denitrification. *Microbiol. Rev.* 46 (1), 43–70.
- Kragh, T., Søndergaard, M., 2004. Production and bioavailability of autochthonous dissolved organic carbon: effects of mesozooplankton. *Aquat. Microb. Ecol.* 36 (1), 61–72.
- Kragh, T., Martinsen, K.T., Kristensen, E., Sand-Jensen, K., 2020. From drought to flood: Sudden carbon inflow causes whole-lake anoxia and massive fish kill in a large shallow lake. *Sci. Total Environ.* 739, 140072 <https://doi.org/10.1016/j.scitotenv.2020.140072>.
- Krijthe, J.H., 2015. (Krijthe): T-Distributed Stochastic Neighbor Embedding using Barnes-Hut Implementation. Retrieved from. <https://github.com/jkrijthe/Rtsn>.
- Kristensen, E., Madsen-Østerby, M., Massicotte, P., Pedersen, O., Markager, S., Kragh, T., 2018. Catchment tracers reveal discharge, recharge and sources of groundwater-borne pollutants in a novel lake modelling approach. *Biogeosciences* 15 (4), 1203–1216. <https://doi.org/10.5194/bg-15-1203-2018>.
- Laird, N.M., Ware, J.H., 1982. Random-effects models for longitudinal data. *Biometrics* 38 (4), 963–974. <https://doi.org/10.2307/2529876>.
- Larned, S.T., 2000. Dynamics of coarse riparian detritus in a Hawaiian stream ecosystem: a comparison of drought and post-drought conditions. *J. N. Am. Benthol. Soc.* 19 (2), 215–234.
- Madsen-Østerby, M., Kragh, T., Pedersen, O., Sand-Jensen, K., 2018. Coupled UV-exposure and microbial decomposition improves measures of organic matter degradation and light models in humic lake. *Ecol. Eng.* 118, 191–200. <https://doi.org/10.1016/j.ecoleng.2018.04.018>.
- Meyer, J.L., Johnson, C., 1983. The influence of elevated nitrate concentration on rate of leaf decomposition in a stream. *Freshw. Biol.* 13 (2), 177–183.
- Moeslund, B., Schläusen, K., Jensen, G., Skovgaard, H., Hermansen, H., Dehli, B., 2018. Anoxia events in streams in the summer of 2018 (in Danish). *Vand Jord* 2018 (3), 109–114.
- Murphy, K.R., Stedmon, C.A., Graeber, D., Bro, R., 2013. Fluorescence spectroscopy and multi-way techniques. *PARAFAC Anal. Methods* 5 (23), 6557–6566. <https://doi.org/10.1039/C3AY4160E>.

- Murphy, K.R., Bro, R., Stedmon, C.A., 2014a. Chemometric analysis of organic matter fluorescence. In: Baker, A., Reynolds, D.M., Lead, J., Coble, P.G., Spencer, R.G.M. (Eds.), *Aquatic Organic Matter Fluorescence*. Cambridge University Press, Cambridge, pp. 339–375.
- Murphy, K.R., Stedmon, C.A., Wenig, P., Bro, R., 2014b. OpenFluor— an online spectral library of auto-fluorescence by organic compounds in the environment. *Anal. Methods* 6 (3), 658–661. <https://doi.org/10.1039/C3AY41935E>.
- Nakagawa, S., Schielzeth, H., 2013. A general and simple method for obtaining R² from generalized linear mixed-effects models. *Methods Ecol. Evol.* 4 (2), 133–142.
- National Geological Survey for Denmark and Greenland, 2015. Surface Geology Map of Denmark 1:25,000, Version 4. Retrieved from: <https://www.geus.dk/produkter-yde-lser-og-faciliteter/data-og-kort/danske-kort/download-jordartskort/>.
- Neilsen, M., 2002. Lowland stream restoration in Denmark: background and examples. *Water Environ. J.* 16 (3), 189–193. <https://doi.org/10.1111/j.1747-6593.2002.tb00393.x>.
- Ogura, N., 1972. Rate and extent of decomposition of dissolved organic matter in surface seawater. *Mar. Biol.* 13 (2), 89–93.
- Pebesma, E., 2018. Simple features for R: standardized support for Spatial Vector Data. *R J.* 10 (1), 439–446. <https://doi.org/10.32614/RJ-2018-009>.
- Pedersen, N.L., Sand-Jensen, K., 2007. Temperature in lowland Danish streams: contemporary patterns, empirical models and future scenarios. *Hydrol. Process.* 21 (3), 348–358. <https://doi.org/10.1002/hyp.6237>.
- Peters, G.T., Webster, J.R., Benfield, E.F., 1987. Microbial activity associated with seston in headwater streams - effects of nitrogen, phosphorus and temperature. *Freshw. Biol.* 18 (3), 405–413. <https://doi.org/10.1111/j.1365-2427.1987.tb01326.x>.
- Pucher, M., 2020. PARAFAC analysis of EEM data to separate DOM components in R. In: *staRdom: spectroscopic analysis of dissolved organic matter in R*. Retrieved from: https://cran.r-project.org/web/packages/staRdom/vignettes/PARAFAC_analysis_of_EEM.html#references. Accessed on March 23th.
- R Core Team, 2018. R: A Language and Environment for Statistical Computing. Retrieved from: <https://www.R-project.org/>.
- Reid, A.J., Carlson, A.K., Creed, I.F., Eliason, E.J., Gell, P.A., Johnson, P.T.J., Kidd, K.A., MacCormack, T.J., Olden, J.D., Ormerod, S.J., Smol, J.P., Taylor, W.W., Tockner, K., Vermaire, J.C., Dudgeon, D., Cooke, S.J., 2019. Emerging threats and persistent conservation challenges for freshwater biodiversity. *Biol. Rev.* 94 (3), 849–873. <https://doi.org/10.1111/brv.12480>.
- Reynolds, D.M., 2002. The differentiation of biodegradable and non-biodegradable dissolved organic matter in wastewaters using fluorescence spectroscopy. *J. Chem. Technol. Biotechnol.* 77 (8), 965–972. <https://doi.org/10.1002/jctb.664>.
- Reynolds, D.M., Ahmad, S.R., 1997. Rapid and direct determination of wastewater BOD values using a fluorescence technique. *Water Res.* 31 (8), 2012–2018. [https://doi.org/10.1016/S0043-1354\(97\)00015-8](https://doi.org/10.1016/S0043-1354(97)00015-8).
- Sand-Jensen, K., Frost-Christensen, H., 1998. Photosynthesis of amphibious and obligately submerged plants in CO₂-rich lowland streams. *Oecologia* 117 (1–2), 31–39. <https://doi.org/10.1007/s004420050628>.
- Sand-Jensen, K., Pedersen, N.L., 2005. Differences in temperature, organic carbon and oxygen consumption among lowland streams. *Freshw. Biol.* 50 (12), 1927–1937. <https://doi.org/10.1111/j.1365-2427.2005.01436.x>.
- Sand-Jensen, K., Pedersen, N.L., Søndergaard, M., 2007. Bacterial metabolism in small temperate streams under contemporary and future climates. *Freshw. Biol.* 52 (12), 2340–2353. <https://doi.org/10.1111/j.1365-2427.2007.01852.x>.
- Sankar, M.S., Dash, P., Lu, Y.H., Mercer, A.E., Turnage, G., Shoemaker, C.M., Chen, S., Moorhead, R.J., 2020. Land Use and Land Cover Control on the Spatial Variation of Dissolved Organic Matter across 41 Lakes in Mississippi. *Hydrobiologia*, USA. <https://doi.org/10.1007/s10750-019-04174-0>.
- Smith, V.H., 2003. Eutrophication of freshwater and coastal marine ecosystems a global problem. *Environ. Sci. Pollut. Res.* 10 (2), 126–139. <https://doi.org/10.1065/espr2002.12.142>.
- Søndergaard, M., Hansen, B., Markager, S., 1995. Dynamics of dissolved organic carbon lability in a eutrophic lake. *Limnol. Oceanogr.* 40 (1), 46–54.
- Stachelek, J., 2019. ipdw: Spatial Interpolation by Inverse Path Distance Weighting. Retrieved from: <https://cran.r-project.org/package=ipdw>.
- Stedmon, C.A., Markager, S., 2005. Resolving the variability in dissolved organic matter fluorescence in a temperate estuary and its catchment using PARAFAC analysis. *Limnol. Oceanogr.* 50 (2), 686–697. <https://doi.org/10.4319/lo.2005.50.2.0686>.
- Stedmon, C.A., Markager, S., Bro, R., 2003. Tracing dissolved organic matter in aquatic environments using a new approach to fluorescence spectroscopy. *Mar. Chem.* 82 (3–4), 239–254. [https://doi.org/10.1016/S0304-4203\(03\)00072-0](https://doi.org/10.1016/S0304-4203(03)00072-0).
- The MathWorks Inc, 2020. MATLAB (Version R2020b).
- Thyssen, N., Erlandsen, M., Jeppesen, E., Ursin, C., 1987. Reaeration of oxygen in shallow, macrophyte rich streams. 1. Determination of the reaeration rate coefficient. *Int. Rev. Gesamten Hydrobiol.* 72 (4), 405–429. <https://doi.org/10.1002/iroh.19870720403>.
- Tiemeyer, B., Freibauer, A., Borraz, E.A., Augustin, J., Bechtold, M., Beetz, S., Beyer, C., Ebli, M., Eickenscheidt, T., Fiedler, S., Förster, C., Gensior, A., Giebels, M., Glatzel, S., Heinichen, J., Hoffmann, M., Höper, H., Jurasinski, G., Lagner, A., Leiber-Sauheitl, K., Peichl-Brak, M., Drösler, M., 2020. A new methodology for organic soils in national greenhouse gas inventories: Data synthesis, derivation and application. *Ecol. Indic.* 109, 105838. <https://doi.org/10.1016/j.ecolind.2019.105838>.
- Verhoeven, J.T., Arheimer, B., Yin, C., Hefting, M.M., 2006. Regional and global concerns over wetlands and water quality. *Trends Ecol. Evol.* 21 (2), 96–103.
- Verhoeven, J.T.A., Meuleman, A.F.M., 1999. Wetlands for wastewater treatment: Opportunities and limitations. *Ecol. Eng.* 12 (1), 5–12. [https://doi.org/10.1016/S0925-8574\(98\)00050-0](https://doi.org/10.1016/S0925-8574(98)00050-0).
- Webster, J., Benfield, E., 1986. Vascular plant breakdown in freshwater ecosystems. *Annu. Rev. Ecol. Syst.* 17 (1), 567–594.
- Weishaar, J.L., Aiken, G.R., Bergamaschi, B.A., Fram, M.S., Fujii, R., Mopper, K., 2003. Evaluation of specific Ultraviolet Absorbance as an Indicator of the Chemical Composition and Reactivity of Dissolved Organic Carbon. *Environ. Sci. Technol.* 37 (20), 4702–4708. <https://doi.org/10.1021/es030360x>.
- Wetzel, R.G., 2001. *Limnology: Lake and River Ecosystems*. Gulf Professional Publishing.
- White, P.A., Kalf, J., Rasmussen, J.B., Gasol, J.M., 1991. The effect of temperature and algal biomass on bacterial production and specific growth rate in freshwater and marine habitats. *Microb. Ecol.* 21 (1), 99–118. <https://doi.org/10.1007/BF02539147>.
- Wickham, H., Bryan, J., Chang, W., LD, McGowan, François, R., Grolemund, G., Hayes, A., Henry, L., Hester, J., Kuhn, M., Pedersen, T.L., Miller, E., Bache, S.M., Müller, K., Ooms, J., Robinson, D., Seidel, D.P., Spinu, V., Takahashi, K., Vaughan, D., Wilke, C., Woo, K., Yutani, H., 2019. Welcome to the {tidyverse}. *J. Open Source Softw.* 4 (43), 1686. <https://doi.org/10.21105/joss.01686>.
- Xu, J., Zhao, Y., Zhao, G., Zhang, H., 2015. Nutrient removal and biogas upgrading by integrating freshwater algae cultivation with piggery anaerobic digestate liquid treatment. *Appl. Microbiol. Biotechnol.* 99 (15), 6493–6501. <https://doi.org/10.1007/s00253-015-6537-x>.